https://doi.org/10.1016/j.compgeo.2019.103375

Use of unsaturated small-strain soil stiffness to the design of wall deflection and ground movement adjacent to deep excavation

Charles Wang Wai Ng, Gang Zheng, Junjun Ni* & Chao Zhou

Charles Wang Wai Ng
CLP Holdings Professor of Sustainability, Department of Civil and Environmental Engineering, the Hong Kong University of Science and Technology, Hong Kong SAR

Gang Zheng
Professor, School of Civil Engineering, Tianjin University, Tianjin, China

Junjun Ni* (corresponding author)
Visiting Assistant Professor, Department of Civil and Environmental Engineering, the Hong Kong University of Science and Technology, Hong Kong SAR

Chao Zhou
Assistant Professor, Department of Civil and Environmental Engineering, the Hong Kong Polytechnic University, Hong Kong SAR

Abstract

Small-strain soil stiffness is an important parameter for the design of wall deflection and ground movements around deep excavations in urban cities. However, the use of unsaturated small-strain soil stiffness in the design of excavation is rarely reported, although the ground condition often becomes unsaturated due to de-watering. The objective of this note is to report and illustrate the effects of suction-dependent small-strain soil stiffness on the design of wall deflection and ground movements due to a 15-m deep excavation in unsaturated soils in Tianjin, China. A small-strain stiffness model for unsaturated soils incorporated into the Hardening Soil-Small Strain (HSS) model was adopted. Two analyses, with and without considering suction-dependent small-strain soil stiffness, were carried out to provide design and construction guidelines to control the progress of excavation. By comparing the measured data with the two different analyses, it is clear that the analysis without considering unsaturated small-strain soil stiffness significantly overestimated the deflection of pile wall by 85%, ground surface settlement by 55% and basement heave by 40%. On the contrary, by considering unsaturated soil stiffness, more accurate predictions were obtained to save construction time and to reduce construction costs.

Keywords: deep excavation, stiffness, suction

1. Introduction

Excavation-induced excessive wall deflection and ground surface settlement can have serious consequences on the surrounding buildings and services. Based on the field data, many empirical and semi-empirical equations, and design charts have been proposed to predict excavation-induced wall deflection and ground surface settlement [1-6]. However, these equations and charts cannot explicitly consider the effects of small-strain soil stiffness and the degree of soil saturation on wall and ground movements. Very often, the initially saturated ground conditions can become unsaturated due to de-watering. Considering the effects of de-saturation of the ground during construction can make economical design analysis of excavation induced wall deflection and ground surface settlement possible.

It is well-known that shear stiffness of saturated soils decreases nonlinearly with an increase in shear strain [7]. For unsaturated soils, small-strain stiffness increases significantly with an increasing suction [8-9]. Over the small strain from 0.001% to 1%, shear stiffness increases by up to 35% when suction increases from 150 to 300 kPa [10]. Furthermore, Ng et al. [11] found that small-strain stiffness is also affected by drying and wetting paths (or hydraulic hysteresis). Ng and Yung [9] proposed semi-empirical equations to simulate small-strain stiffness of unsaturated soils as a power function of net stress and soil suction. However, the use of these equations in design analysis is rarely reported.

In this technical note, the use of suction-dependent small-strain soil stiffness in the design analysis of a 15-m deep excavation in Tianjin, China is reported. In the design analyses, a Hardening Soil-Small Strain (HSS) model [12] was modified by incorporating suction effects on soil stiffness into Plaxis 2D [13]. To ensure safety and economical construction progress, field measurements were compared with numerical predictions with and without considering suction-dependent small-strain soil stiffness during the excavation throughout.

2. The excavation project

2.1 Construction site

The excavation project for the high-rise buildings, approximately 181 m by 268 m on plan, is situated in the downtown area of Tianjin, China (Fig. 1). The northern side was retained by 29 m-long contiguous piles (each diameter of 0.9 m at 1.1 m spacing), whereas the other three sides were supported by diaphragm walls with a thickness of 1 -1.2 m. In the northern side, an earth berm (19 m in width and 11.5 m in height) was cut in front of the pile wall to provide extra support during excavation (Fig. 2(a)). At the inner boundary of the earth berm, two-row 21 m-long contiguous piles with row spacing of 3.2 m were installed (Fig. 2(b)).

2.2 Soil profile and properties

In the excavation site, there were three different soil types (i.e., fill, silt and silty clay) along the depth (Fig. 2(b)). The top 5.5 m layer was fill material. The soil at depths of 9.5-11.5 m and 23.0-24.2 m was classified as silt. Soil at other depths was classified as silty clay. In order to determine the basic properties of the soils, intact soil samples were collected from the field for laboratory triaxial and oedometric tests [14]. The properties of these three soils are summarised in Table 1.

3. Numerical analysis

Plane-strain design analyses were carried out using the finite element software Plaxis 2D. In the analysis, a typical section in the northern side of excavation (labelled as A-A, Fig. 2(a)) was selected. Effective stress analysis was adopted under fully drained condition. Two analyses, with and without considering suction-dependent soil stiffness were conducted.

3.1 Finite element mesh and boundary conditions

Figure 2(b) shows the finite element mesh adopted in the analyses. According to Zheng et al. [14], the soil was modelled using fifteen-node triangular elements, whereas the contiguous piles were simulated using plate elements. The thickness of the plates was estimated based on the equivalent values of the flexible stiffness [15]. Both the horizontal and vertical displacements at the bottom boundary were fixed. At the two lateral boundaries, a vertical sliding boundary was set with rollers, whereas the the horizontal displacement was constrained. The ground water tables inside and outside the excavation were set at depths of -17.2 m and -3 m, respectively. No slip elements were used at the soil-wall interface. That means the soil elements adjacent to the pile wall were directly connected to the pile wall surface. The numerical convergence was ensured by using a Newton-type iterative procedure [13].

3.2 Constitutive model

The HSS constitutive model developed by Benz [12] was used in the analysis. In the model, there are two main parameters controlling small strain soil stiffness, namely initial shear stiffness G_0 and a reference shear strain $\gamma_{0.7}$ at which shear stiffness is 70% of G_0. HSS model can account for the the reduction of shear stiffness with increasing strain at small strains. Finite element analyses using HSS model have been demonstrated to be able to predict the deformation of soils and retaining structures during excavation [14, 16-17].

Ng and Yung [9] derived a small-strain stiffness model for unsaturated soils by accounting for both net stress and soil suction

$$G_0 = C^2 f(e)\left(\frac{p}{p_{ref}}\right)^{2n}\left(1+\frac{s}{p_{ref}}\right)^{2k} \quad (1)$$

where C is a constant reflecting the inherent soil structure; $f(e)$ is a void ratio function relating shear stiffness to void ratio, and this function can adopt the formulation e^a for simplicity, where a is a regression parameter; p and s are mean net stress and matric suction (u_a-u_w), respectively; p_{ref} is reference pressure for normalizing p and generally assumed as 1 kPa for simplicity; n and k are regression parameters.

By coupling HSS constitutive model and Ng and Yung [9] model in this study, the effects of suction and strain on small-strain soil stiffness were incorporated in finite element simulation.

3.3 Input parameters for soil and pile wall

The parameters *C*, *a*, *n* and *k* required by equation (1) were determined based on the experimental data by the least-squares method using a multiple linear regression model [9]. They were calibrated to be 65.5, -0.77, 0.17 and 0.045, respectively, for both silt and silty clay. For simplicity, the above calibrated parameters were also applied for the fill material. Young's modulus, Poisson' ratio and unit weight of the pile wall were 30 GPa, 0.2 and 25 kN/m^3, respectively. A summary of other measured parameters used in the HSS model is given in Table 1.

3.4 Construction stages and simulation procedures

The simulation procedures were in accordance with the actual construction stages. The initial stress conditions of soils in the simulation were generated at 1 g (gravitational acceleration) by assuming that the coefficient of at-rest earth pressure of soil (K_0) is equal to 1-sinφ' [18]. At construction Stage 1, the installation of the contiguous piles was modelled with a "wish-in-place" (WIP) wall for simplicity [19]. Then, the plate elements of the contiguous piles were activated. At Stage 2, water table inside the excavation was lowered down to the depth of -17.2 m. From Stage 3 to Stage 6 (final stage), the ground was consecutively excavated to the depths of -2 m, -3.7 m, -10.45 m and -15.2 m, respectively. The suction distribution above the ground water table during excavation was assumed to follow the hydrostatic line. Excavation was simulated by removing nodes and elements in each stage.

4. Comparison of analyses with and without considering suction effects on soil stiffness

4.1 Deflection of pile wall

Figure 3(a) shows the comparison of the measured and predicted wall deflection without considering suction effects on small-strain soil stiffness. It can be seen that a cantilever mode of wall deflection was measured and predicted after each excavation stage. From construction Stage 3 to the final stage, the magnitude of wall deflection increased, especially near the ground surface. The measured maximum lateral wall deflection was around 0.3% of excavation depth. This value is much smaller than Peck's data (2% of excavation depth; Peck [1]), where there were lateral supporting systems. It implies that without using the lateral supporting systems in the current project, the presence of unsaturated earth berm in front of pile wall could also reduce the wall deflection significantly.

The analysis without considering unsaturated soil stiffness shows that the predicted results were larger than the measured data, especially at Stage 5 and final stage. At the end of excavation, wall deflection near ground surface was overestimated by 85%. However, the prediction used to control construction was improved significantly when considering the effects of soil suction on soil stiffness in the model (Fig. 3(b)). The analysis considering soil suction effects predicted the wall deflection quite well at Stage 3. The prediction error was only 20% at the final stage. The comparison between Figs 3(a) and Fig. 3(b) reveals that the wall deflection was highly overestimated when soil stiffness was determined from saturated soils. It also demonstrates the importance of modelling suction-dependent small-strain soil stiffness in the design analysis of deep excavations.

4.2 Ground surface settlement

Figure 4(a) shows the comparison of the ground surface settlement behind the pile wall by using saturated soil stiffness. Based on the field measurement, the maximum surface settlement after the final stage was 46.5 mm (around 4 m away from the wall). The predicted results reveal that with the increase of distance from pile wall, the ground surface settlement increased first and then decreased gradually. The maximum ground surface settlement was located at a distance of 2.5 m away from the back of the wall. A concave type of settlement profile was observed. The analysis based on saturated soil stiffness shows that the maximum settlement at final stage was highly overestimated by 55%. On the contrary, the analysis predicted the ground surface settlement quite well when the unsaturated soil stiffness was considered (see Fig. 4(b)). Suction induced increase in soil stiffness of earth berm restrained the lateral wall deflection (Fig. 3) and hence reduced the ground surface settlement behind the wall. By comparing Figs 4(a) and Fig. 4(b), it is revealed that the prediction of ground surface settlement without considering unsaturated soil stiffness was too conservative and hence not economical in practical design.

4.3 Basement heave

Figure 5 shows the basement heave during excavation. The measured maximum heave was 43 mm, which was around 4 m away from the inner pile wall. The predicted results clearly show that the basement heave was in convex shape, with the maximum value at about 3 m away from the pile wall. The heave amount became constant, when the distance away from the pile wall was more than 20 m. Compared to the analysis based on saturated soil stiffness, the analysis considering suction-dependent soil stiffness could better predict the maximum basement heave. The accuracy of prediction was improved by more than 40%, when suction effects were considered. This improvement demonstrates that the unsaturated soil within the top 2 m of the basement could restrict the ground heave due to the suction induced increase in small-strain soil stiffness.

Based on the predicted and measured results in Figures 3-5, it is clear that the design analysis with suction-dependent small-strain soil stiffness properly predicted the field performance due to de-watering in deep excavation. Hence, the analysis considering unsaturated soil stiffness provided a safe and economical design during construction. It saved construction time and reduced construction costs.

5. Conclusions

By considering suction-dependent small strain stiffness to account for the effects of de-watering in design analyses of a 15-m deep excavation in Tianjin, China, wall deflection and ground movements were predicted and compared with field measurements during the construction of the excavation. It can be concluded the analysis without considering unsaturated small-strain soil stiffness significantly overestimated the deflection of pile wall by 85%, the ground surface settlement by 55% and basement heave by 40%. On the contrary, by considering unsaturated soil stiffness, the analysis allowed for safe and economical design and construction of the deep excavation. It is recommended that unsaturated small-strain soil stiffness should be considered due to de-watering during the construction of deep excavations in the short-term.

Acknowledgements

The authors acknowledge the research grant 16212218 provided by the Research Grants Council of HKSAR.

References

[1] Peck RB. Deep excavation and tunneling in soft ground, In: Proceedings of the 7th International Conference on Soil Mechanics and Foundation Engineering, state-of-the-art volume, Mexico City, 1969: 225–290.

[2] Hsieh PG, Ou CY. Shape of ground surface settlement profiles caused by excavation. Can Geotech J 1998; 35(6): 1004–1017.

[3] Liu GB, Ng CWW, Wang ZW. Observed performance of a deep multistrutted excavation in Shanghai soft clays. J Geotech Geoenviron Eng ASCE 2005; 131(8): 1004–1013.

[4] Leung EHY, Ng CWW. Wall and ground movements associated with deep excavations supported by cast-in-situ wall in mixed ground conditions. J Geotech

Geoenviron ASCE 2007; 133(2): 129–143.

[5] Wang J, Xu Z, Wang W. Wall and ground movements due to deep excavations in Shanghai soft soils. J Geotech Geoenviron Eng ASCE 2010; 136(7): 985–994.

[6] Tan Y, Wei B. Observed behaviors of a long and deep excavation constructed by cut-and-cover technique in Shanghai soft clay. J Geotech Geoenviron Eng ASCE 2012; 138(1): 69–88.

[7] Atkinson JH. Non-linear soil stiffness in routine design. Géotechnique 2013; 50(5): 487–507.

[8] Mancuso C, Vassallo R, d'Onofrio A. Small strain behavior of a silty sand in controlled-suction resonant column - torsional shear tests. Can Geotech J 2002; 39(1): 22–31.

[9] Ng CWW, Yung SY. Determination of the anisotropic shear stiffness of an unsaturated decomposed soil. Géotechnique 2008; 58(1): 23–35.

[10] Ng CWW, Xu J. Effects of current suction ratio and recent suction history on small-strain behaviour of an unsaturated soil. Can Geotech J 2012; 49(2): 226–243.

[11] Ng CWW, Xu J, Yung SY. Effects of wetting-drying and stress ratio on anisotropic stiffness of an unsaturated soil at very small strains. Can Geotech J 2009; 46(9): 1062–1076.

[12] Benz T. Small-strain stiffness of soil and its numerical consequences. Ph.D. thesis, University of Stuttgart, Germany; 2007.

[13] Brinkgreve RBJ, Kumarswamy S, Swolfs WM. PLAXIS version 2015 Manual. The Netherlands; 2015.

[14] Zheng G, Yang X, Zhou H, Du Y, Sun J, Yu X. A simplified prediction method for evaluating tunnel displacement induced by laterally adjacent excavations. Comput Geotech 2018; 95: 119–128.

[15] Chai JC, Shrestha S, Hino T, Ding WQ, Kamo Y, Carter J. 2D and 3D analyses of an embankment on clay improved by soil–cement columns. Comput Geotech 2015; 68: 28–37.

[16] Kung GTC, Ou CY, Juang CH. Modeling small-strain behavior of Taipei clays for finite element analysis of braced excavations. Comput Geotech 2009; 36(1): 304–319.

[17] Zhang WG, Goh ATC, Xuan F. A simple prediction model for wall deflection caused by braced excavation in clays. Comput Geotech 2015; 63: 67–72.

[18] Jáky J. The coefficient of earth pressure at rest. Journal for the Society of Hungarian Architects and Engineers 1944; 7: 355-358.

[19] Ng CWW. Nonlinear modelling of wall installation effects. Retaining structures, Thomas Telford, London, 1993:160-163.

Figure

(a)

Figure 1 Overview of the excavation site in Tianjin, China

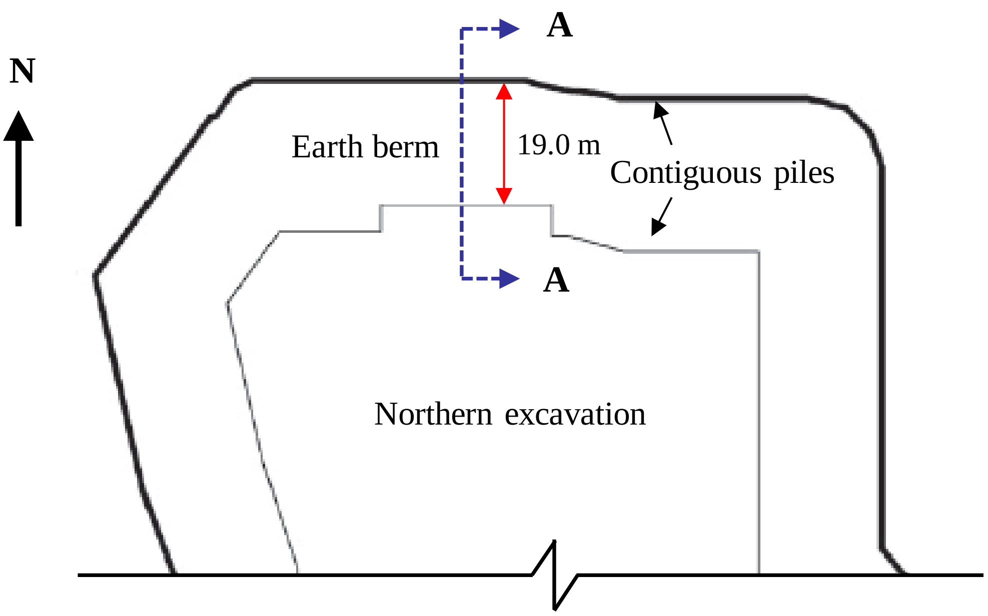

(a)

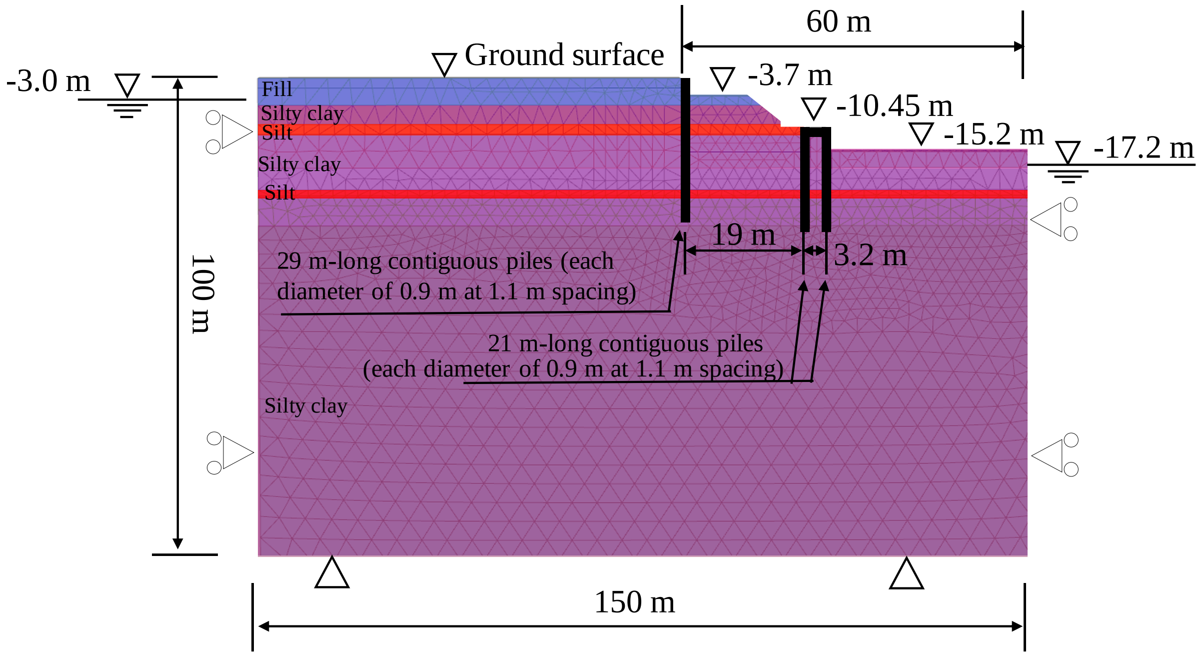

(b)

Figure 2 (a) Location of the selected cross-section A-A and (b) illustration of cross-section A-A of the excavation in the design analysis

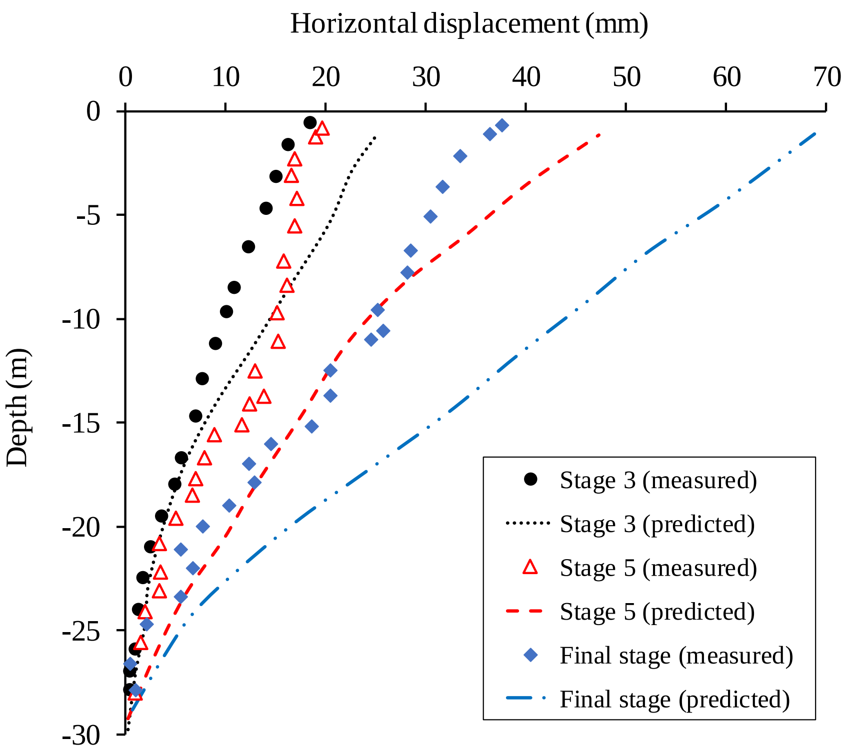

(a)

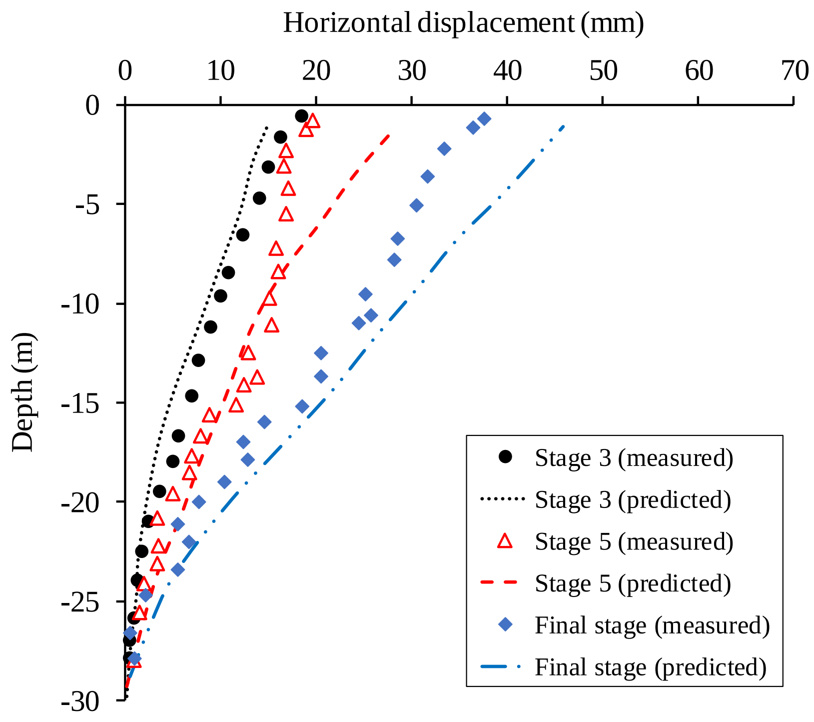

(b)

Figure 3 Comparison between measured and predicted deflection of pile wall: (a) without and (b) with considering suction-dependent soil stiffness

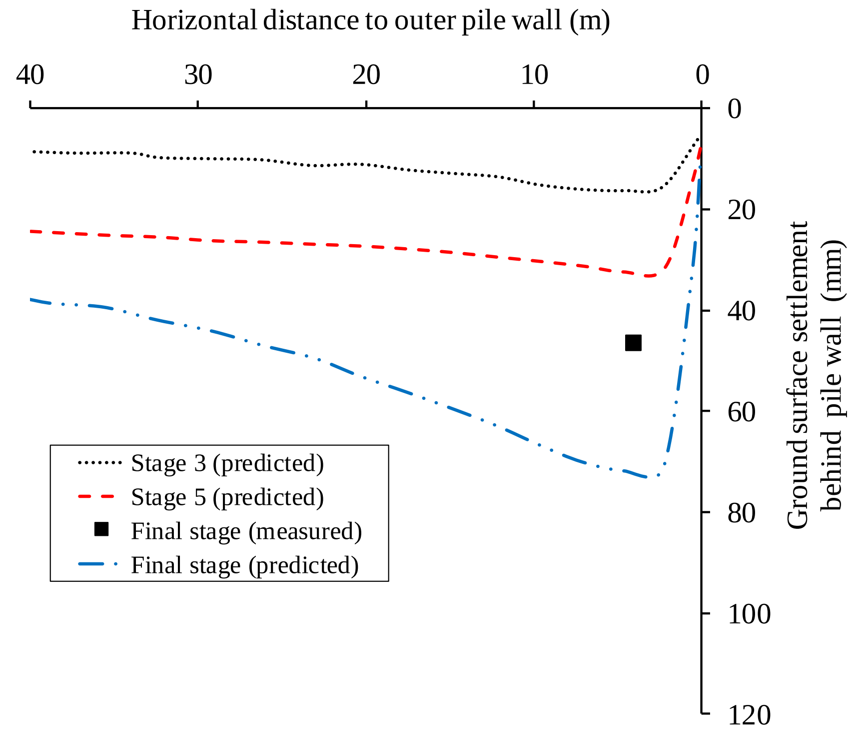

(a)

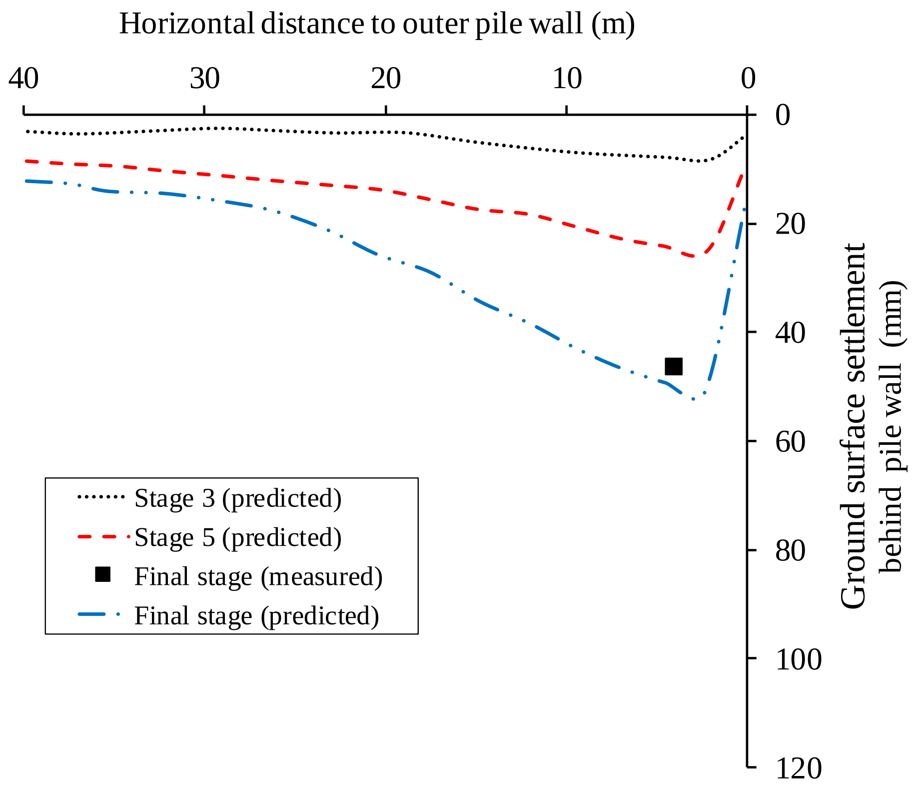

(b)

Figure 4 Comparison between measured and predicted ground surface settlement after outer pile wall: (a) without and (b) with considering suction-dependent soil stiffness

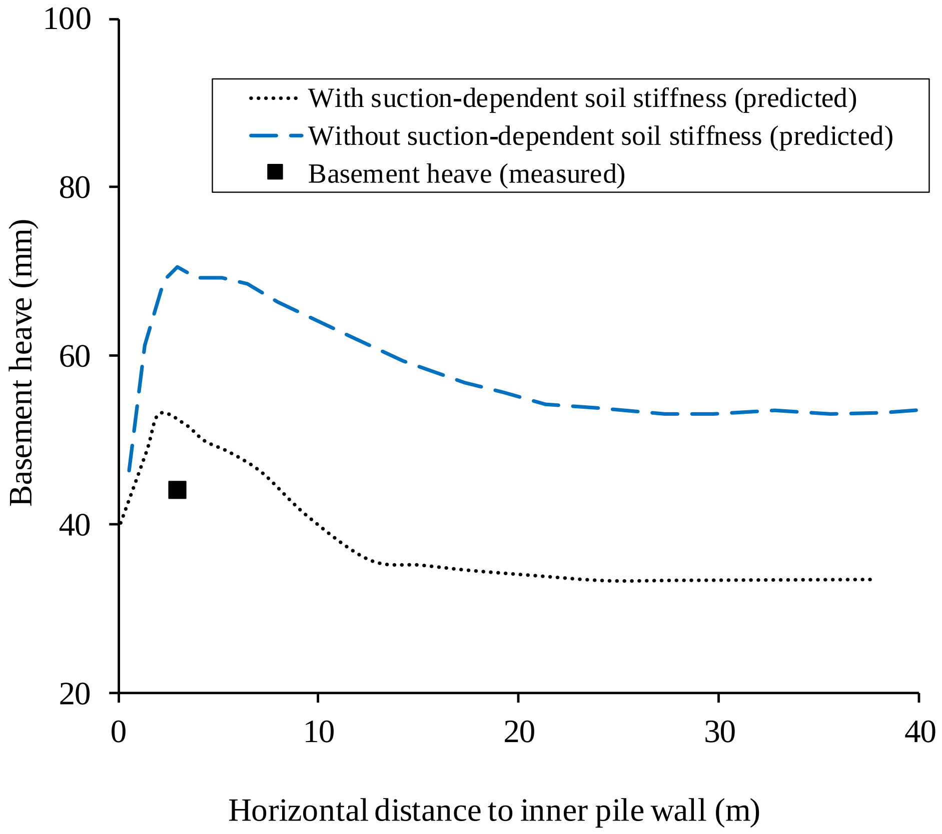

Figure 5 Comparison between measured and predicted basement heave with and without considering suction-dependent soil stiffness

Table

Table 1 Soil parameters used in the design analysis

	Soil depth (m)	γ *(kN/m³)*	*e*	*c' (kPa)*	*φ'* (°)	E_{50}^{ref} *(MPa)*	E_{oed}^{ref} *(MPa)*	E_{ur}^{ref} *(MPa)*	G_0 * *(MPa)*	$\gamma_{0.7}$
Fill	0-5.5	18.5	0.94	12	16.1	4.4	4.4	26.3	71.0	0.0002
Silt	9.5-11.5 23.0-24.2	18.7	0.74	10	32.3	8.4	8.4	44.1	119.2	0.0002
Silty clay	5.5-9.5 11.5-23.0 >24.2	19.8	0.64	14	25.7	7.2	5.1	36.8	99.3	0.0002

Note: In the table, γ is unit weight of soil; *e* is void ratio; *c'* is effective cohesion; *φ'* is effective friction angle; E_{50}^{ref} is triaxial loading Young's modulus when shear stress is 50% of shear strength; E_{oed}^{ref} is oedometric loading modulus; E_{ur}^{ref} is unloading–reloading Young's modulus; G_0 is initial shear stiffness and $\gamma_{0.7}$ is a reference shear strain at which shear stiffness is 70% of G_0.

*These values for G_0 do not consider suction-dependent soil stiffness. In the analysis with considering suction dependency, G_0 was calculated using equation (1).